RGNZ/MGPB

Impact of the Layering of Blast-Induced Damage Factors in the Hoek–Brown Failure Criterion on the Bench Damage Monitoring of Mines

Seyed Ahmad Mousavi[1]; Kaveh Ahangari[2]; Kamran Goshtasbi[3]

[1] Department of Mining Engineering, Science and Research Branch, Islamic Azad University, Tehran, Iran,
   ORCID http://orcid.org/0000-0001-6152-7744

[2] Department of Mining Engineering, Science and Research Branch, Islamic Azad University, Tehran, Iran,
   ORCID http://orcid.org/0000-0001-9462-7303

[3] Mining Engineering Department, Tarbiat Modares University, Tehran, Iran, ORCID http://orcid.org/0000-0003-1202-3536

Abstract

The process of creating a slope in a rock mass using the excavation and blasting methods consistently leads to stress release in the rock mass, resulting in a certain level of fracture and disturbance. Blast-induced vibrations can also influence the quality of the rock mass remaining after the blasting, as well as the stability and bench damage monitoring (BDM) of mines. A damage factor (D) is included in the Hoek–Brown failure criterion to compute the disturbance of a rock mass in creating a slope. Choosing the value and thickness of the blast zone for the Hoek–Brown criterion is crucial in the safety analysis and BDM of mines. However, the selection is still a crucial technical challenge in this criterion. Employing nonlinear layering, the present study divides the rock mass behind a blast hole into several layers with decreasing D values applied to each layer. The numerical simulation was conducted using the FLAC finite difference software for bench vibration assessment and damage monitoring by checking the peak particle velocity (PPV) in the bench face with different geometries. Behind the blast hole, five different layers of D were considered through which the Hoek–Brown properties of the rock mass declined nonlinearly during the execution of the model. Since the disturbance threshold of PPV was assumed to be 120 mm/s, the toe and middle parts of the small benches were in the disturbance threshold, while for the medium and high benches, only the bench toe was within the disturbance threshold.

Keywords:
Hoek-Brown failure criterion; damage factor; bench damage monitoring; peak particle velocity; rock slope geometry

1. Introduction

Seismic vibrations or waves caused by blasts are among the significant issues and consequences of blasting in mines. The waves may result in the opening and slippage of joints and faults, damage to benches and surrounding structures, and environmental and economic problems (**Kutter and Fairhurst, 1971; Haghnejad et al., 2019**). Unwanted damages to benches and slopes are categorized as blast-induced rock mass damages. These damages lower the rock mass integrity, on the one hand, and cause excavation problems, slope instability, and inappropriate reduction of the bench width, on the other hand. Hence, the control of ground vibrations, calculation of the damage thickness in the rock mass, and minimization of the blast-induced damages are of great significance (**Saiang, 2010; Silva et al., 2019; Behera and Dey, 2022**). A ground vibration, occurring in a fraction of a second, stimulates a rock mass's mechanical and dynamic properties. The impacts of an explosion in a

single-hole can be divided into the following four stages, as shown in **Figure 1** (**Shadabfar et al., 2020**):
- expansion of the blast hole,
- formation of a crushed zone surrounding the blast hole,
- penetration of radial cracks through the rock mass and formation of a cracked zone,
- creation of ground vibrations under the influence of blast-induced waves.

Numerous studies have been performed on damage estimation in rock and soil masses. Generally, the methods can be classified as analytical, numerical, or empirical (**Yang et al., 2020; Wei et al., 2021**).

Analytical methods use parameters such as peak particle velocity (PPV), borehole pressure, or explosion pressure as critical factors to estimate the size of a damage zone (**Ma et al., 2011; Gharehgheshlagh and Alipour, 2020; Pan et al., 2020; Shadabfar et al., 2020; Behera and Dey, 2022**). In numerical methods, algorithms such as the finite element method (FEM), finite difference method (FDM), and discrete element method (Shadabfar et al.) are employed to evaluate the damages

Corresponding author: Kaveh Ahangari

e-mail address: kaveh.ahangari@gmail.com
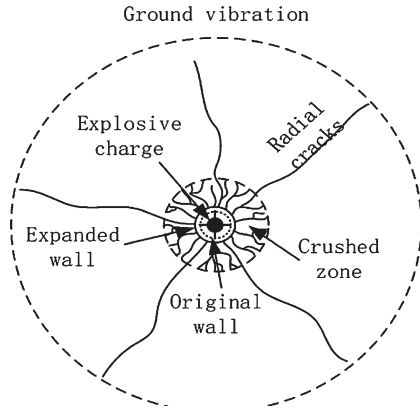
Figure 1: The zones surrounding a blast hole (**Shadabfar et al., 2020**)

Figure 2: The linear reduction in D in each layer of the blast damage (**Zheng et al., 2018**)

and stress field variations around a blast hole and study the resultant issues (**Lupogo et al., 2014; Wang et al., 2018; Chen et al., 2019; Haghnejad et al., 2019; Afrasiabian et al., 2020; Yari et al., 2022**). An empirical relationship is created through several laboratory or in-situ tests for estimating the damage size and the rock mass properties in a blast-induced zone (**Persson, 1997; Hoek and Karzulovic, 2000; Sheng et al., 2002; Mesec et al., 2017; Qian et al., 2017; Stanković et al., 2017; Zheng et al., 2018**). Some empirical criteria, such as the Hoek–Brown failure criterion, have been suggested to rapidly estimate the rock mass parameters (**Hoek and Brown, 1980; Renani and Cai, 2021**). A parameter called the damage factor had been consequently introduced to enhance the strength estimation accuracy of a rock mass regarding blast-induced strength reduction and stress relaxation during excavations. This factor allows for the rapid estimation of the rock mass properties in a blast damage zone (**Hoek and Brown, 1980; Hoek et al., 2002; Hoek and Diederichs, 2006; Hoek and Brown, 2019; Zuo and Shen, 2020**).

In the guideline of the Hoek-Brown failure criterion, a constant disturbance factor (D=0.5, 0.7, 1.0) is assigned to rock masses regardless of the damage reduction with the rise in the depth behind slope surfaces and holes (**Hoek et al., 2002; Hoek, 2012; Hoek and Brown, 2019**). Some researchers have suggested assigning a variable disturbance factor to the area behind the slope surfaces since assigning a constant disturbance factor to a damaged area is inappropriate. For instance, some researchers have proposed a decremental damage factor and a parallel layer model (PLM), as shown in **Figure 2**, to create a more logical and accurate model (**Li et al., 2011; Lupogo et al., 2014; Qian et al., 2017; Rose et al., 2018; Yilmaz et al., 2018; Zheng et al., 2018**). Some other researchers have used the quantitative value of the blast damage factor for numerical modeling (**Hamdi et al., 2011; Wang et al., 2018; Chen et al., 2019; Pan et al., 2020; Yang et al., 2020; Mousavi et al., 2022**). Therefore, dividing a rock mass slope into several layers with decremental values of D applied to each behind the hole is better to have a more realistic
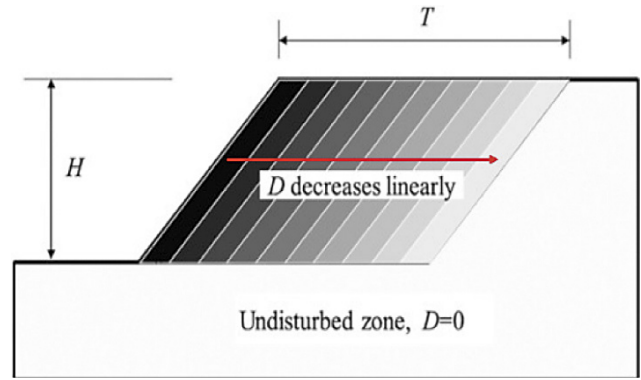
model. The present study used the empirical criterion of Persson damage to determine the thickness of blast-induced damages and layering of D around the hole. Eventually, bench damage monitoring (BDM) was performed using a PPV threshold and the numerical simulation in the finite difference FLAC software.

2. Theoretical background

2.1. Relationship between Hoek–Brown failure criterion and the damage zone of a rock mass

From 1980 to 2018, the Hoek-Brown failure criterion for rock mass has been updated to several editions, and its concepts and equations have been fundamentally changed. The following equation (**Equation 1**) is the current expression of this criterion (**Hoek and Brown, 2019**):

$$\sigma_1 = \sigma_3 + \sigma_{ci}\left(m_b \frac{\sigma_3}{\sigma_{ci}} + s\right)^a \tag{1}$$

Where:
σ_1 – major principal stress (Mpa),
σ_3 – minor principal stress (Mpa),
σ_{ci} – uniaxial compressive strength of the intact rock mass (Mpa).

In addition, m_b, s, and a are the Hoek-Brown constants for the rock mass and can be calculated using the following equations (**Equations 2-4**):

$$m_b = m_i \exp\left(\frac{GSI - 100}{28 - 14D}\right) \tag{2}$$

Where:
m_i – Hoek-Brown constant for intact rock,
GSI – the geological strength index,
D – the blast damage factor,
m_b – Hoek–Brown constant for rock mass.

$$s = \exp\left(\frac{GSI - 100}{9 - 3D}\right) \tag{3}$$

Where:
s – Hoek–Brown constant for rock mass.

$$a = \frac{1}{2} + \frac{1}{6}(e^{-GSI/15} - e^{-20/3}) \qquad (4)$$

Where:

a – Hoek–Brown constant for rock mass.

For intact rock, s=1 and a=0.5, and D is a factor that depends upon the degree of disturbance from a blast or stress relaxation. The value of D varies from 0 for undisturbed in situ rock masses to 1 for very disturbed rock masses. As Hoek et al. suggested, **Equations 5** and **6** can be applied to estimate the compressive and tensile strengths of the rock mass, and these equations are expressed as follows:

$$\sigma_{cm} = \sigma_{ci} \times \frac{(m_b + 4s - a(m_b - 8s))(m_b / 4 + s)^{a-1}}{2(1+a)(2+a)} \qquad (5)$$

$$\sigma_{tm} = \frac{s\sigma_{ci}}{m_b} = \frac{\sigma_{ci}}{m_i} \cdot \exp\left[\frac{(GSI - 100).(19 - 11D)}{(9 - 3D).(28 - 14D)}\right] \qquad (6)$$

And disturbed rock mass deformation modulus is expressed as the **Equation 7**:

$$E_{rm} = E_i(0.02 + \frac{1 - D/2}{1 + e^{((60 + 15D - GSI)/11)}}) \qquad (7)$$

Where:

E_i – the elastic modulus of intact rock (MPa),

E_{rm} – the deformation modulus of rock mass (MPa).

The modulus of deformation (E_{rm}), m_b, and s of a rock mass are among the parameters directly related to the damage factor in the Hoek-Brown failure criterion (**Hoek et al., 2002; Hoek and Diederichs, 2006**). With the increment of D, these parameters decline, resulting in the indirect reduction in the compressive and tensile strengths of the rock mass. Hoek et al. provided preliminary guidelines for determining the value and thickness of the disturbance factor D based on qualitative criteria, such as the excavation method and rock mass surface shape when evaluating the rock mass disturbance level. However, damages caused by blasting excavation will change with an increase in depth from the rock surface. Hence, the disturbance factor will also alter with depth.

2.2. Relationship between PPV and the damage zone of a rock mass

A blast-induced damage zone is where new cracks occur, and old ones propagate. The most common approach to determine the blast-induced damages is to numerically or empirically measure the blast-induced vibrations. Most of the empirical damage criteria have been proposed based on PPV, which is referred to as the peak value of the vector resulting from three components, i.e. the longitudinal, vertical, and transversal velocity, as shown in **Equation 8** (**Afrasiabian et al., 2020**):

$$PPV = \sqrt{(V_{max})_x^2 + (V_{max})_y^2 + (V_{max})_z^2} \qquad (8)$$

Where:

PPV – peak particle velocity (mm/s),

V_x – the longitudinal velocity (mm/s),

Vy – the vertical velocity (mm/s),

V_z – the transversal velocity (mm/s).

Different empirical relationships have been proposed so far for the estimation of PPV. Holmberg and Persson (1978) introduced the Swedish approach to determine a damage zone, estimate particle velocity, and obtain the radius of the damage zone (**Holmberg and Persson, 1978**). They proposed **Equation 9** to assess blast-induced damages as follows:

$$PPV = \frac{KQ^\alpha}{R^\beta} \qquad (9)$$

Where:

Q – explosive charge weight (kg),

R – distance from the charge (m),

K, α, β – site-specific constants.

The PPV threshold is remarkably affected by the characteristics of a blasting load and the rock mass properties. Therefore, it is hard to obtain an accurate threshold value. Many researchers have used PPV in field tests and numerical analyses to study the damage threshold and proposed different values and standards for the threshold (**Singh and Narendrula, 2004; Wei et al., 2009; Lu et al., 2012; Pan et al., 2020**). In this regard, Persson (2009) proposed **Table 1** to estimate the damage to a rock mass based on induced PPV (**Persson, 1997**).

Table 1: Damage criterion of a hard rock mass (**Persson, 1997**)

Typical effect	PPV (mm/s)
Incipient swelling	700
Incipient damage	1000
Fragmentation	2500
Good fragmentation	5000
Crushing	15000

Based on a set of experiments, Persson found that the PPV in the region 700 to 1000 mm/s begins to give measurable damage in the form of slight swelling and slightly decreased shear strength. Velocities in the region of 2500 mm/s are characteristic of the range where fragmentation begins. Velocities around 5000 mm/s are characteristic of very good fragmentation, whereas velocities in the neighbourhood of 15000 mm/s are required to crush the rock mass (**Persson, 1997**). Furthermore, in Persson et al. (**Persson et al., 1993**), the relation between PPV and materials properties is given by **Equation 10** to estimate the threshold of critical peak particle velocity:

$$PPV_{crit} = \frac{\sigma_t C_p}{E} \qquad (10)$$

Where:

PPV$_{crit}$ – threshold of critical peak particle velocity (mm/s),

C_p – the compression velocity (mm/s),

σ_t – the tensile strength (Pa).

2.3. Theoretical considerations on the dynamic analysis of the blast

In the dynamic analysis of the blast, specific considerations and points, such as blast loading, how to apply boundary conditions, the model's damping, and wave transition in the model should be noted. Through the blasting procedure, the surrounding rock mass of blast hole is approximately loaded in two stages. At first, the loading is conducted by the impact wave. Then, the expansion caused by the explosion gases results in the reloading on the surrounding rock mass of the blast hole. Experimental methods can be beneficial in estimating the charge-generated pressure. The magnitude of shock wave pressure is a function of the velocity of detonation, density, and charge ingredients. Various researchers provided several equations to apply blast hole pressure dynamically. **Equations 11 to 14** are widely used to calculate the maximum dynamic pressure applied to the wall of the blast chamber (blast hole pressure). The merit of these functions is that they use rock mass properties and explosives to calculate blast hole pressure (**Haghnejad et al., 2019; Afrasiabian et al., 2020**).

$$PD = 432 \times 10^{-6} \times \rho_e \left(\frac{VD^2}{1 + 0.8\rho_e} \right) \qquad (11)$$

Where:

PD – blasting pressure (MPa),

ρ_e – explosive density (g/cm^3),

VD – detonation velocity (m/s).

$$PE = \frac{1}{2} PD \qquad (12)$$

Where:

PE – the pressure gas (MPa).

$$PW = PE.\left(\frac{r_h}{b} \right)^{-qk} \qquad (13)$$

Where:

PW – pressure behind the hole (MPa),

r_h – hole radius (Chamanzad and Nikkhah),

b – explosive radius (Chamanzad and Nikkhah),

q – specific heat coefficient,

k – explosive shape factor (2 for cylindrical charges and 3 for spherical charges).

$$P(t) = PW.\frac{8\rho_r.C_p}{\rho_r.C_p + VD.\rho_e} \left[e^{(-Bt/\sqrt{2})} - e^{(-\sqrt{2}Bt)} \right]$$
$$\& \quad B = 16338 \qquad (14)$$

Where:

P(t) – dynamic pressure (MPa),

ρ_r – rock density (g/cm^3),

VD – detonation velocity (m/s),

t – time (s).

In addition, appropriate boundary conditions, mechanical damping, and damping ratio should be considered to avoid the unwanted reflection of the blasting wave within the model and absorb the energy of the input body wave. In dynamic problem analysis, any artificial boundary causes the generated waves to reflect into the calculation field after reaching these boundaries; however, in real conditions, these waves can propagate and get absorbed within the infinite field without reflecting into the calculation field. Many researchers have worked to solve this problem. Quiet (viscous) boundary and free-field boundary conditions are two methods to apply boundary conditions. Lysmer and Kuhelemeyer presented the employed method in finite difference software. This method introduces independent dashpots in boundary grid points that cause the energy of the input body wave to be almost completely absorbed with no reflection. Quiet boundaries are best suited when the dynamic source is applied within the model. On the other hand, since every mechanical system has internal damping, the vibration of this system continues forever if there is no damping. Therefore, a necessary consideration in the dynamic analysis is to assign mechanical damping and its corresponding ratio. Rayleigh and hysteretic damping are two types of damping that can be considered for the model. In addition, the damping ratio is usually around 2 to 5% and 2 to 10% for geological materials and structural systems, respectively. In analyses where the plasticity constitutive model is applied, a considerable amount of energy dissipation is lost in the plastic flow. Therefore, only a small percentage of damping, e.g. 0.5%, is required for most dynamic analyses that include large strains (**Itasca, 2012**).

On the other hand, one of the important issues concerning meshing in dynamic analyses is determining the proper mesh size to control wave transmission. The frequency and velocity of a wave applied to the system are two characteristics affecting the numerical computation accuracy of wave propagation. As recommended by Kuhelemeyer and Lysmer (**Kuhlemeyer and Lysmer, 1973**), the reasonable and accurate analysis of the wave propagation in the numerical space and ensuring the proper transmission of waves requires the size of elements (Δl) to be within 0.1 to 0.125 of the wavelength associated with the highest frequency component of the input wave that contains appreciable energy (**Itasca, 2012**). That is:

$$\lambda/10 \le \Delta l \le \lambda/8 \qquad (15)$$

Where:

Δl – the element size (m),

λ – the wavelength (m).

3. Methodology

The disturbance factor D cannot be comprehensively obtained solely based on the excavation method and rock mass surface shape and as mentioned in the Introduction, in a numerical simulation, the disturbance factor should not be taken as a constant value between zero and one. Instead, it should be considered layering behind a slope surface or using the quantitative equations available. Accordingly, the present study suggests the nonlinear layering of the Hoek-Brown damage factor based on the empirical criterion of Persson (see **Table 1**), as shown in **Table 2**. To this end, five nonlinear layers were considered for D (D=0, 0.1, 0.3, 0.7, 1.0). That is, in FLAC Software, the FISH program is first used to scan all zones of the model, the PPV of each zone is determined based on **Equation 8**, and the value of D is assigned for each zone, according to the PPV of that particular zone. Then, all Hoek-Brown parameters related to the damage factor, including bulk modulus, shear modulus, m_b and s of the rock mass, were reduced during the run only in the layering of the damaged zones. Consequently, the compressive and tensile strengths of the rock mass (σ_c and σ_t, respectively) were updated. This is the merit of this method over the one weakening the whole model.

**Table 2:** The suggested blast damage factor layering

Damage factor (D)	PPV (mm/s)
0	<700
0.1	700-900
0.3	900-1000
0.7	1000-2500
1.0	>2500

Therefore, after applying the blasting load to the model and updating the parameters of the Hoek-Brown failure criterion in the damaged zone in the form of nonlinear layering, PPV monitoring for BDM was performed using the FISH programming in FLAC software for the considered recorded points.

3.1. The model geometry and properties

For bench damage monitoring (BDM), first, monitoring goals should be determined regarding the requirements of rock engineering challenges and the use of microseismic monitoring. Then, the whole region involved can be evaluated based on monitoring goals. The sensitivity extension and location accuracy in the monitored

zones depend on the possibility and severity of the rock mass instability in each zone. Microseismic monitoring should be more sensitive and have higher location accuracy in cases with a higher likelihood of rock mass instability. According to the International Society for Rock Mechanics (ISRM), in slope engineering monitoring, sensors are directly installed on the slope body, where the slope surface concerns exist (**Xiao et al., 2016**). Thus, in this study, the monitoring was performed on the slope's toe, middle, and crest. The total number of created models was 90, which included three benches of 5, 10, and 15 meters in height and three slope angles of 55°, 65°, and 75°, and various widths (the distance between the hole and the toe of the bench above) from 1 to 10 meters, which are schematically shown in **Figure 3**.
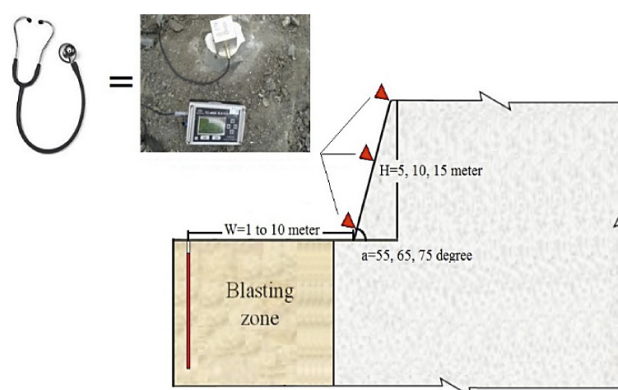
Figure 3: The geometric variables of the bench and monitoring points of PPV

The rock mass properties were also extracted from the values presented by Hoek and Brown for granites (**Hoek and Brown, 1997**). The modified Hoek-Brown model was used to model the rock mass behaviour. **Table 3** lists the rock mass properties.

3.2. Damp, mesh, and boundary conditions

According to the geomechanical parameters of the surrounding rock mass of blast hole, the shear and compression wave velocities (m/s) are computed using **Equations 16** and **17** as follows (**Kuhlemeyer and Lysmer, 1973; Itasca, 2012**):

$$C_S = \sqrt{\frac{G}{\rho}} \qquad (16)$$

Where:
C_s – S-wave velocity (m/s),
G – the shear modulus (Pa),
ρ – density of the rock mass (kg/m³).

Table 3: Dynamic properties of a granite rock mass (**Hoek and Brown, 1997**)

D	Density(kg/m³)	m_i	GSI	m_b	s	a	σ_{tm} (Pa)	σ_{cm} (Pa)	E_{rm} (Pa)
0	2700	25	75	10.23	0.062	0.501	1.69E+06	1.28E+08	8.16E+10
1	2700	25	75	4.19	0.015	0.501	1.03E+06	7.96E+07	2.70E+10

$$C_P = \sqrt{\frac{K + 4G/3}{\rho}} \qquad (17)$$

Where:

C_p – P-wave velocity (m/s),
K – the bulk modulus (Pa).

By substituting the elastic properties of the most critical state of the surrounding rock mass of blast hole, i.e. the rock mass properties corresponding with D=1 from **Table 3** in the equations above, the compressive and shear wave velocities were calculated at 3333.33 and 2041.24 m/s, respectively. The mesh size was calculated to be about 2 meters based on **Equation 15**, and was considered a smaller mesh size, i.e. 0.5 meters, to gain more accuracy in dynamic blast modeling. The unlimited (viscous) boundary conditions and Rayleigh damping were employed to avoid unwanted reflection of the blasting wave into the model and absorption of the input body wave energy. Furthermore, a damping ratio of 0.5% was used (**Itasca, 2012**).
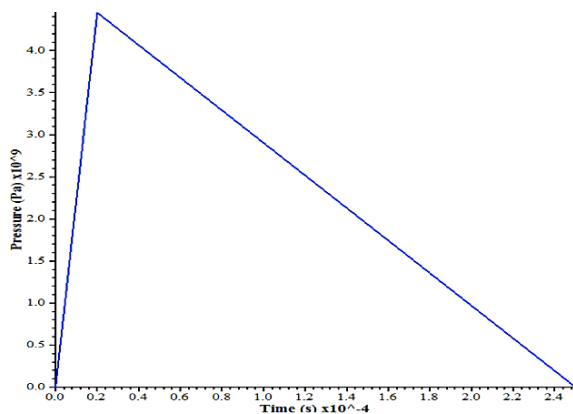
3.3. Blast loading

A single-hole with a diameter of 200 mm and a burden of 2 meters was considered in this study. The explosive was ANFO, with a detonation velocity of 4160 m/s and an explosive density of 0.931 g/cm³ (**Grisaro and Edri, 2017**). The maximum dynamic pressure was calculated to be 4.45 GPa using the pressure function in **Equation 14**. Since explosive blasting is a complex instantaneous process (**Chen et al., 2019**), so as to simplify the analysis in this study, the blasting load was applied as a triangle pulse time history curve to the model. As shown in **Figure 4**, the dynamic load resulting from the explosion of ANFO was applied to the hole wall in the form of a stress wave with a rise time of 20 s after 250 μs with a maximum value of 4.45 GPa.

4. Results and discussion

In the present study, three different models were developed: models with constant Hoek-Brown parameters of D=0 and D=1 (based on **Table 3**) and a model applying the layering (D=Layering) according to **Table 2**. The PPV values from the hole-head to the toe of the above bench (history points from a to u) with a spacing of 50 cm were monitored. **Figure 5** demonstrates the PPV values for a model with a height of 5 m, slope angle of 55°, and width of 10 m for ten points on the ground surface. As can be seen, the PPV value decreases with the rise in the distance from the hole, indicating wave damping. **Figure 6** compares the PPV values for the three models with D=0, D=1, and D=Layering. The values recorded for the model with D=0 are lower than those for the model with D=1. In the model where D was assigned in the form of layering, the recorded values differ from those of the two mentioned models. This indicates that weakening the model's mechanical properties by apply-
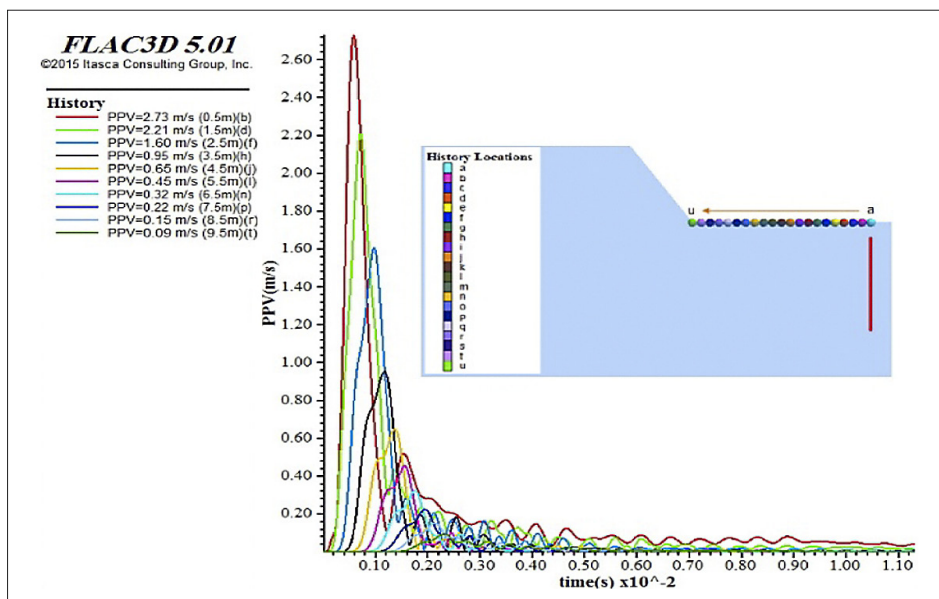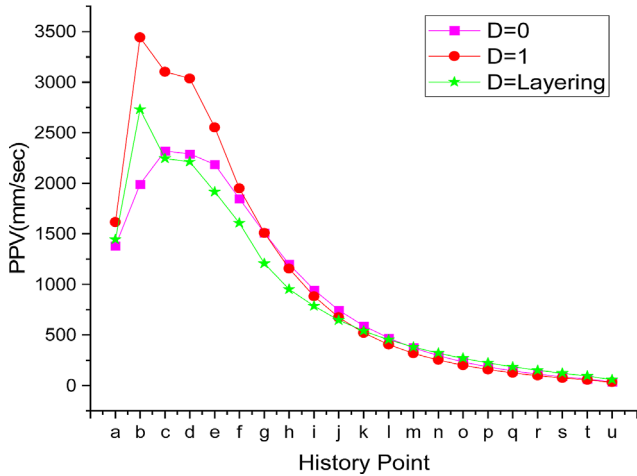

Figure 4: Time history diagram of the equivalent load
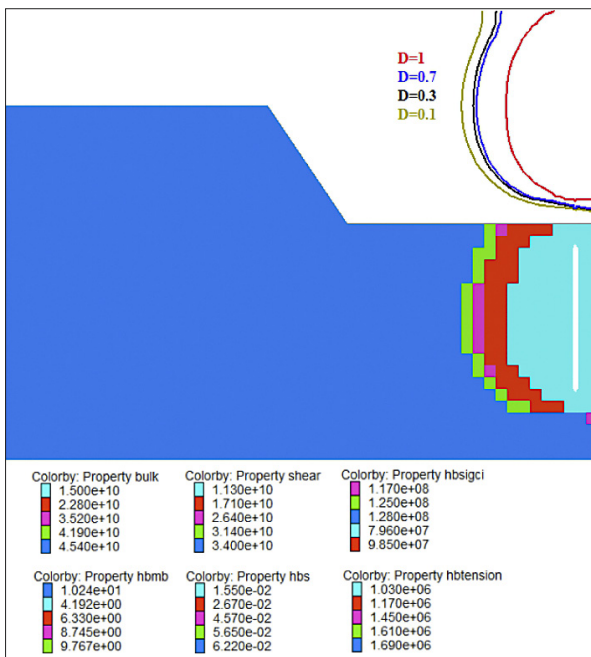

Figure 5: The PPV recorded in a model with D=Layering

Figure 6: The PPVs recorded in two models of rock masses with D=0 and D=1, compared to a model with D= layering

ing D=1 results in higher vibration values in the model. This weakening may have lower correctness regarding numerical modeling, i.e. underestimating the rock mass's stability and strength. Therefore, by assigning layering to D in the model and allowing it to apply the D value during the run and lower other parameters depending on the D of Hoek-Brown criterion only for the damaged area, more reasonable values of the PPV are obtained. Accordingly, the other models were developed by applying the layering for D.

4.1. Effect of the blast-induced vibration on the rock mass properties

The initial values of the dynamic properties of the rock, i.e. D=0, shown in **Table 3**, were applied to the

model. Then, D was applied as layering. The zones of the model where PPV equaled 700 mm/s were considered blast-induced damage zones. Thus, all mechanical parameters of the rock mass (such as deformation modulus, m_b, s, compressive strength and tensile strength), which are input properties of the modified Hoek-Brown constitutive model, were updated for each zone during each timestep by FISH programming in the FLAC software. These parameters were reduced only in the damaged zone, and the initial values of properties (D=0) were preserved in other zones.

Figure 7 illustrates the Hoek-Brown disturbance factor due to the explosion behind the blasting hole in five layers. As can be seen, in damaged zones around the hole, where the blasting energy is tremendous, the bulk and shear moduli of the rock mass decline, and as the distance from the hole increases, they increase to the undamaged values. The reduction in the m_b *(hbmb)*, s *(hbs)*, σ_{cm} *(hbsigci)* and σ_{tm} *(hbtension)* properties of Hoek–Brown between the damaged and undamaged rock masses are also shown in the form of layering.

4.2. Fracture propagation around the blast hole

The plastic region around the hole can be used as a separate criterion for understanding rock mass fracture

Figure 7: The reduction in rock mass properties in the damaged region
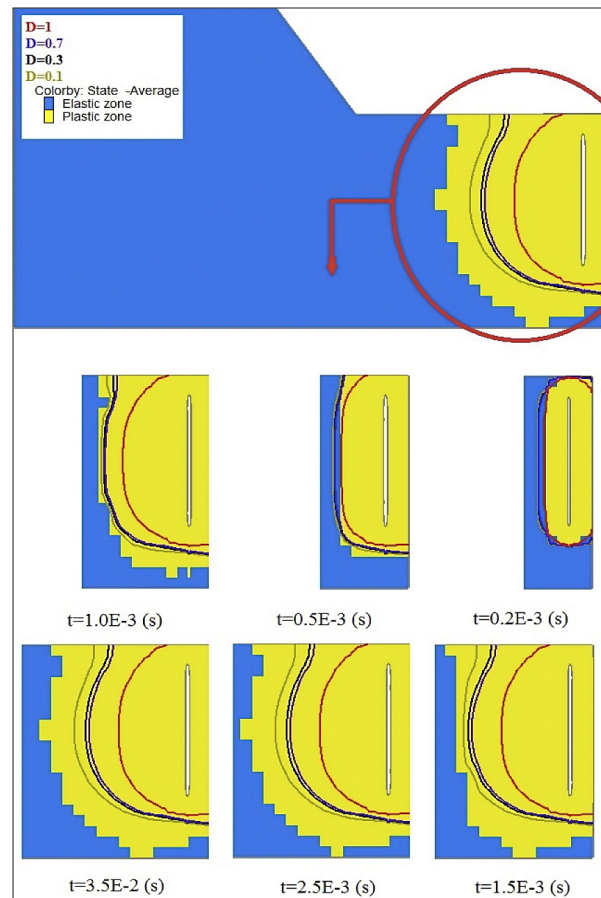
Figure 8: A comparison between the plastic zone and D layering around the hole
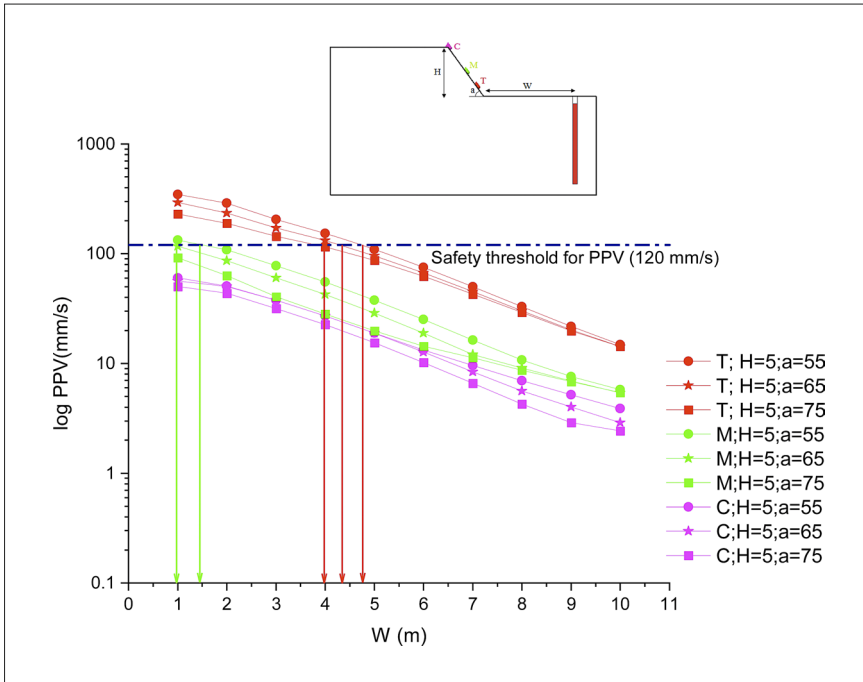
Figure 9: PPV (mm/s) values recorded in the toe, middle, and crest of short benches
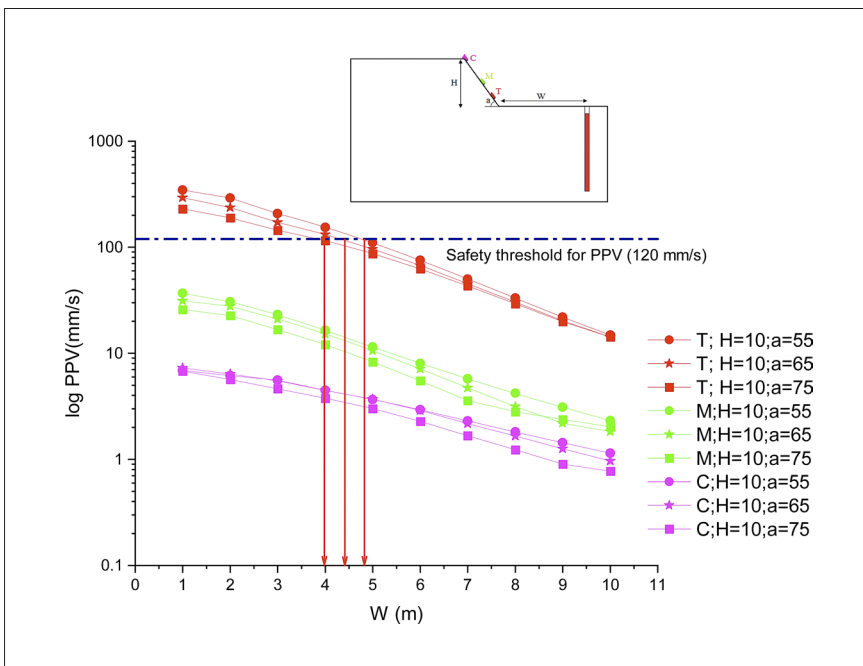
Figure 10: PPV (mm/s) values recorded in the toe, middle, and crest of medium benches

behaviour due to blast damage. The plastic zones around the hole indicate regions where stresses meet the failure criterion. The plastic yield indicates the maximum value of the cracking numerically.

The plastic zone plotted in **Figure 8** can be compared with the Hoek-Brown disturbance factors shown as contours. The model was executed until the input wave was thoroughly damped. This was achieved by recording the velocity history at different points. The plastic zone was compared with the Hoek-Brown damage layering at different points until the run was over. The Hoek-Brown damage layering was found to have approximately equal sizes with the plastic zone. In time 0.2E-3 s, when the

blasting began, the plastic zone radius equaled 1 m, and the Hoek-Brown damage layering was 1.3 m. At the end of the execution, the radius of the plastic zone equaled 6 m (30 times the hole diameter), and the radius of the Hoek-Brown layering equaled 4.9 m (25 times the hole diameter).

4.3. Evaluation of the bench damage monitoring (BDM)

The PPV, the most common index for judging the amount of rock mass damage, was used for BDM with geometric properties shown in **Figure 5**. **Figures 9-11**
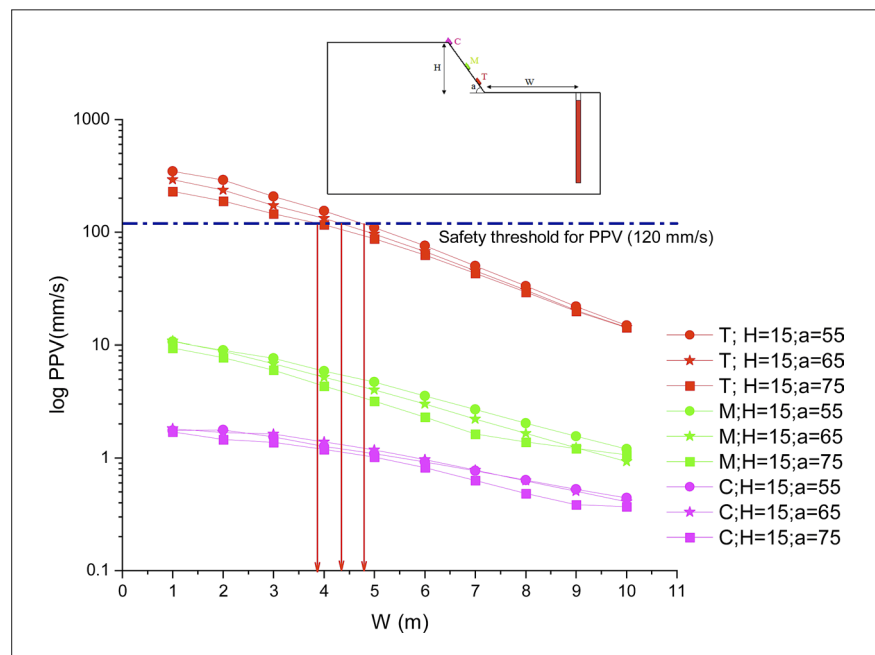
Figure 11: PPV (mm/s) values recorded in the toe, middle, and crest of high benches

illustrate the PPV variations in bench face at three points, i.e. the crest (C), middle (M), and toe (T) of a bench with different heights (H), slope angles (a), and widths (distance between the hole and the bench toe, W). **Figures 9-11** illustrate the short benches (H=5 m), medium benches (H=10 m), and high benches (H=15 m), respectively. The history point was also considered 1 meter above the bench toe.

As is evident, the PPV values decrease gradually with the rise in the distance from the blast hole. That is, for higher blasting energies (shorter distances to the blasting hole), PPV values increased, while for lower blasting energies (longer distances from the blasting hole), PPV values decreased. The maximum and minimum values of PPV were recorded in the toe and the crest, respectively. As stated, different values of critical PPV have been proposed by researchers to determine the damage threshold in the form of tables and standards. The present study employed the equation suggested by Persson et al. (**Persson et al., 1993**) (**Equation 10**) to calculate the safe distances and BDM. By substituting the values of **Table 3** in **Equation 10**, the critical PPV was obtained at almost 120 mm/s. Thus, this value was chosen as the damage threshold and shown with horizontal dashed lines in the figures.

As shown in **Figure 9**, for small benches (H=5 m), two parts, i.e. the toe and middle, will be subjected to the damage threshold. Therefore, it can be interpreted that if the distance between the single-hole and the top bench is about 1.5 m, the effect of vibration and damage will reach the middle of the top bench. Moreover, it can be seen that within distances shorter than 5 m from the top bench, the toe of the top bench will be subject to damage threshold. Therefore, in the present study that investigates the blasting impact of a single-hole on its top

bench, either the blast load should be decreased, or the distance from the blast hole should be extended to more than 5 m to gain safety for the three positions of the top bench, i.e. the crest, toe, and middle, and avoid any damages to these positions. In addition, as shown in **Figures 10** and **11**, only the toe of the top bench will be in the damage threshold in medium (H=10 m) and high (H=15 m) benches. Furthermore, the present study investigated the blasting impact of a single-hole on its top bench with three typical slope angles of 55°, 65°, and 75°. PPV values are lower for steeper slopes (75°) in constant blasting energies (constant distance between the hole and bench) and are higher for smoother slopes (55°). As a matter of fact, the blast-resulted vibration is greater in smoother slopes compared to steeper slopes. Moreover, the results indicate that changes within this range of slope angle are less affected by the recorded value of PPV and vibration in the slope face, compared to changes in the bench height.

5. Conclusions

The Hoek-Brown failure criterion estimates the damage factor (D) using a descriptive approach, and it is hard to calculate this factor precisely. Considering constant D value for the whole model is a common mistake in modeling. The present study used Persson's empirical damage criterion to determine the damage thickness and D layering around the hole. The blasting process of a granite rock slope was numerically simulated using the modified Hoek-Brown failure criterion in the finite difference FLAC software. Eventually, BDM was analyzed using the PPV threshold.

According to the numerical simulation results, applying the blasting load to the rock mass led to the increased

slope damage factor over time and, finally, a damage zone around the blasting hole. The mechanical properties of the Hoek-Brown behavioural model, as well as the rock mass quality, lowered due to the nonlinear reduction of D in the form of layering caused by receding from the hole. The numerical simulation revealed that using different rock mass properties in the blasting zone yielded different results in the PPV evaluation of the slope compared to using a constant D value. Regarding the threshold PPV analysis, high blasting energy caused by a closer hole to the top bench can cause severe damage to the slope face. The bench became safer by reducing the blasting energy, i.e. increasing the hole's distance from the slope face. Since the damage threshold of PPV was considered 120 mm/s, the toe and middle of the benches were within the damage threshold for small benches, while for the medium and high benches, only the bench toe was within the damage threshold. The PPV values were lower for steeper slopes in constant blasting energies (constant distance between the hole and top bench) and higher for smoother slopes.

6. References

Afrasiabian, B., Ahangari, K. and Noorzad, A. (2020): Study on the effects of blast damage factor and blast design parameters on the ground vibration using 3D discrete element method. Innovative Infrastructure Solutions, 5(2), 1-14. https://doi.org/10.1007/s41062-020-0286-0.

Behera, S. and Dey, K. (2022): A PPV-Based Prediction Model to Construct Damage Envelop for Crater Blasts. Journal of The Institution of Engineers (India): Series D, 103(1), 13-23. https://doi.org/10.1007/s40033-021-00294-x.

Chamanzad, M.A. and Nikkhah, M. (2020): Sensitivity Analysis of Stress and Cracking in Rock Mass Blasting using Numerical Modelling. Journal of Mining and Environment, 11(4), 1141-1155.

Chen, Y., Xu, J., Huo, X. and Wang, J. (2019): Numerical simulation of dynamic damage and stability of a bedding rock slope under blasting load. Shock and Vibration, 2019. https://doi.org/10.1155/2019/9616859.

Gharehgheshlagh, H.H. and Alipour, A. (2020): Ground vibration due to blasting in dam and hydropower projects. Rudarsko-geološko-naftni zbornik, 35(3). https://doi.org/10.17794/rgn.2020.3.6.

Grisaro, H.Y. and Edri, I.E. (2017): Numerical investigation of explosive bare charge equivalent weight. International Journal of Protective Structures, 8(2), 199-220. https://doi.org/10.1177/2041419617700256.

Haghnejad, A., Ahangari, K., Moarefvand, P. and Goshtasbi, K. (2019): Numerical investigation of the impact of rock mass properties on propagation of ground vibration. Natural Hazards, 96(2), 587-606. https://doi.org/10.1007/s11069-018-3559-6.

Hamdi, E., Romdhane, N.B. and Le Cléac'h, J.-M. (2011): A tensile damage model for rocks: application to blast induced damage assessment. Computers and Geotechnics,

38(2), 133-141. https://doi.org/10.1016/j.compgeo.2010.10.009.

Hoek, E. (2012): Blast damage factor D. Technical note for RocNews, 1-7.

Hoek, E. and Brown, E. (2019): The Hoek–Brown failure criterion and GSI–2018 edition. Journal of Rock Mechanics and Geotechnical Engineering, 11(3), 445-463. https://doi.org/10.1016/j.jrmge.2018.08.001.

Hoek, E. and Brown, E.T. (1980): Empirical strength criterion for rock masses. Journal of the geotechnical engineering division, 106(9), 1013-1035. https://doi.org/10.1061/AJGEB6.0001029.

Hoek, E. and Brown, E.T. (1997): Practical estimates of rock mass strength. International journal of rock mechanics and mining sciences, 34(8), 1165-1186.

Hoek, E., Carranza-Torres, C. and Corkum, B. (2002): Hoek-Brown failure criterion-2002 edition. Proceedings of NARMS-Tac, 1(1), 267-273.

Hoek, E. and Diederichs, M.S. (2006): Empirical estimation of rock mass modulus. International journal of rock mechanics and mining sciences, 43(2), 203-215. https://doi.org/10.1016/j.ijrmms.2005.06.005.

Hoek, E. and Karzulovic, A. (2000): Rock mass properties for surface mines. Slope Stability in Surface Mining, WA Hustrulid, MK McCarter and DJA van Zyl, Eds, Society for Mining, Metallurgical and Exploration (SME), Littleton, CO, 59-70.

Holmberg, R. and Persson, P.A. (1978): The Swedish approach to contour blasting, SveDeFo.

Itasca, F. (2012): Fast Lagrangian Analysis of Continua in 3-Dimension (FLAC3D V 5.01). Itasca Consulting Group: Minneapolis, MN, USA.

Kuhlemeyer, R.L. and Lysmer, J. (1973): Finite element method accuracy for wave propagation problems. Journal of the Soil Mechanics and Foundations Division, 99(5), 421-427. https://doi.org/10.1061/JSFEAQ.0001885.

Kutter, H. and Fairhurst, C. (1971): On the fracture process in blasting. International Journal of Rock Mechanics and Mining Sciences & Geomechanics Abstracts, 8(3), 181-202. https://doi.org/10.1016/0148-9062(71)90018-0.

Li, A., Merifield, R. and Lyamin, A. (2011): Effect of rock mass disturbance on the stability of rock slopes using the Hoek-Brown failure criterion. Computers and Geotechnics, 38(4), 546-558. https://doi.org/10.1016/j.compgeo.2011.03.003.

Lu, W.B., Luo, Y., Chen, M. and Shu, D.Q. (2012): An introduction to Chinese safety regulations for blasting vibration. Environmental Earth Sciences, 67(7), 1951-1959. https://doi.org/10.1007/s12665-012-1636-9.

Lupogo, K., Tuckey, Z., Stead, D. and Elmo, D. (2014): Blast damage in rock slopes: potential applications of discrete fracture network engineering. Proceedings of the 1st International Discrete Fracture Network Engineering Conference, Vancouver, Canada. p, 14.

Ma, G., Hao, H. and Wang, F. (2011): Simulations of explosion-induced damage to underground rock chambers. Journal of Rock Mechanics and Geotechnical Engineering, 3(1), 19-29. https://doi.org/10.3724/SP.J.1235.2011.00019.

Mesec, J., Strelec, S. and Težak, D. (2017): Ground vibrations level characterization through the geological strength index (GSI). Rudarsko-geološko-naftni zbornik, 32(1), 1-6. https://doi.org/10.17794/rgn.2017.1.1.

Mousavi, S.A., Ahangari, K. and Goshtasbi, K. (2022): An Investigation into Bench Health Monitoring under Blast Loading in Hoek-Brown Failure Criterion using the Finite Difference Method. Journal of Mining and Environment. https://doi.org/10.22044/jme.2022.12094.2207.

Pan, Q., Zhang, J. and Zheng, S. (2020): Study on distribution characteristics of damage range along smooth blasting hole based on PPV. Mathematical Problems in Engineering, 2020. https://doi.org/10.1155/2020/4785839.

Persson, P.A. (1997): The relationship between strain energy, rock damage, fragmentation, and throw in rock blasting. Fragblast, 1(1), 99-110. https://doi.org/10.1080/13855149709408392.

Persson, P.A., Holmberg, R. and Lee, J. (1993): Rock Blasting and Explosives Engineering. CRC Press.

Qian, Z., Li, A.J., Lyamin, A. and Wang, C. (2017): Parametric studies of disturbed rock slope stability based on finite element limit analysis methods. Computers and Geotechnics, 81, 155-166. https://doi.org/10.1016/j.compgeo.2016.08.012.

Renani, H.R. and Cai, M. (2021): Forty-Year Review of the Hoek–Brown Failure Criterion for Jointed Rock Masses. Rock Mechanics and Rock Engineering, 1-23. https://doi.org/10.1007/s00603-021-02661-2.

Rose, N., Scholz, M., Burden, J., King, M., Maggs, C. and Havaej, M. (2018): Quantifying transitional rock mass disturbance in open pit slopes related to mining excavation. Proceedings of the XIV International Congress on Energy and Mineral Resources.

Saiang, D. (2010): Stability analysis of the blast-induced damage zone by continuum and coupled continuum–discontinuum methods. Engineering Geology, 116(1-2), 1-11. https://doi.org/10.1016/j.enggeo.2009.07.011.

Shadabfar, M., Gokdemir, C., Zhou, M., Kordestani, H. and Muho, E.V. (2020): Estimation of damage induced by single-hole rock blasting: A review on analytical, numerical, and experimental solutions. Energies, 14(1), 29. https://doi.org/10.3390/en14010029.

Sheng, Q., Yue, Z., Lee, C., Tham, L. and Zhou, H. (2002): Estimating the excavation disturbed zone in the permanent shiplock slopes of the Three Gorges Project, China. International Journal of Rock Mechanics and Mining Sciences, 39(2), 165-184. https://doi.org/10.1016/S1365-1609(02)00015-1.

Silva, J., Worsey, T. and Lusk, B. (2019): Practical assessment of rock damage due to blasting. International Journal of Mining Science and Technology, 29(3), 379-385. https://doi.org/10.1016/j.ijmst.2018.11.003.

Singh, S. and Narendrula, R. (2004): Assessment and prediction of rock mass damage by blast vibrations. Proc. Conference on Mine Planning and Equipment Selection MPES.

Stanković, S., Dobrilović, M. and Bohanek, V. (2017): A practical approach to the ground oscillation velocity measurement method. Rudarsko-geološko-naftni zbornik, 32(4), 55-61. https://doi.org/10.17794/rgn.2017.4.6.

Wang, Y., Wang, S., Zhao, Y., Guo, P., Liu, Y. and Cao, P. (2018): Blast induced crack propagation and damage accumulation in rock mass containing initial damage. Shock and Vibration, 2018. https://doi.org/10.1155/2018/3848620.

Wei, D., Chen, M., Lu, W. and Wang, Z. (2021): Failure Mechanism of Back-Break in Bench Blasting of Thin Terrane. Applied Sciences, 11(6), 2577. https://doi.org/10.3390/app11062577.

Wei, X., Zhao, Z. and Gu, J. (2009): Numerical simulations of rock mass damage induced by underground explosion. International Journal of Rock Mechanics and Mining Sciences, 46(7), 1206-1213. https://doi.org/10.1016/j.ijrmms.2009.02.007.

Xiao, Y.X., Feng, X.T., Hudson, J.A., Chen, B.R., Feng, G.L. and Liu, J.P. (2016): ISRM suggested method for in situ microseismic monitoring of the fracturing process in rock masses. Rock Mechanics and Rock Engineering, 49(1), 343-369. https://doi.org/10.1007/s00603-015-0859-y.

Yang, J., Dai, J., Yao, C., Jiang, S., Zhou, C. and Jiang, Q. (2020): Estimation of rock mass properties in excavation damage zones of rock slopes based on the Hoek-Brown criterion and acoustic testing. International Journal of Rock Mechanics and Mining Sciences, 126, 104192. https://doi.org/10.1016/j.ijrmms.2019.104192.

Yari, M., Ghadyani, D. and Jamali, S. (2022): Development of a 3D numerical model for simulating a blast wave propagation system considering the position of the blasting hole and in-situ discontinuities. Rudarsko-geološko-naftni zbornik, 38(2), 68-78. https://doi.org/10.17794/rgn.2022.2.6.

Yilmaz, M., Ertin, A., Er, S. and Tugrul, A. (2018): Numerical modelling of steep slopes in open rock quarries. Journal of the Geological Society of India, 91(2), 232-238. https://doi.org/10.1007/s12594-018-0841-x.

Zheng, H., Li, T., Shen, J., Xu, C., Sun, H. and Lü, Q. (2018): The effects of blast damage zone thickness on rock slope stability. Engineering Geology, 246, 19-27. https://doi.org/10.1016/j.enggeo.2018.09.021.

Zuo, J. and Shen, J. (2020): The Hoek-Brown Failure Criterion--From Theory to Application. Singapore, Springer.

SAŽETAK

Utjecaj raslojavanja čimbenika oštećenja izazvanih miniranjem u Hoek-Brownovu kriteriju sloma na praćenje oštećenja etaža u kopovima

Proces stvaranja kosina u stijenskoj masi metodama iskopa i miniranja dovodi do oslobađanja naprezanja u stijenskoj masi, što rezultira određenom razinom loma i oštećenja. Vibracije izazvane miniranjem također mogu utjecati na kvalitetu minirane stijenske mase, kao i na stabilnost i praćenje oštećenja etaža (BDM) površinskoga kopa. Koeficijent poremećenosti stijenske mase (D) uključen je u Hoek-Brownov kriterij sloma za izračunavanje oštećenja stijenske mase pri izradi kosine. Odabir vrijednosti i širine zone miniranja prema Hoek-Brownovu kriteriju ključan je u analizi sigurnosti i BDM-a kopova. Međutim, odabir još uvijek predstavlja ključni tehnički izazov. Koristeći se nelinearnom slojevitošću, ova analiza dijeli stijensku masu iza minske bušotine u nekoliko slojeva sa smanjivanim vrijednostima D za pojedini sloj. Numerička simulacija provedena je korištenjem softvera FLAC za procjenu vibracija na etažama i praćenje oštećenja provjerom vršne brzine čestica (PPV) na etaži s različitim geometrijama. Iza minske bušotine razmatrano je pet različitih nizova D kroz koje su Hoek-Brownova svojstva stijenske mase nelinearno mijenjana tijekom analize modela. Budući da je granična vrijednost PPV-a pretpostavljena na 120 mm/s, vrh i središnji dijelovi malih etaža bili su na graničnoj vrijednosti oštećenja, dok je za srednje i visoke etaže samo vrh etaže bio unutar granične vrijednosti oštećenja.

Ključne riječi:
Hoek-Brownov kriterij sloma, koeficijent poremećenosti stijenske mase, praćenje oštećenja na etaži, maksimalna brzina čestice, geometrija kosine stijene

Author's contribution

Seyed Ahmad Mousavi (1) (PhD candidate) carried out the numerical simulation and provided analyses, writing, presentation and interpretation of the results. **Kaveh Ahangari (2)** (Full Professor at the Faculty of Engineering) proposed the key ideas and contributed to the methodology, interpretation, and analyses of the results. **Kamran Goshtasbi (3)** (Full Professor at the Faculty of Engineering) managed the whole process and supervised it from the beginning to the end.